

1 **Early epidemiological assessment of the transmission**
2 **potential and virulence of coronavirus disease 2019**
3 **(COVID-19) in Wuhan City: China, January-February,**
4 **2020**

5 **Authors:** Kenji Mizumoto^{1,2,3} §, Katsushi Kagaya^{2,4}, Gerardo Chowell³

6 **Affiliations:**

7 ¹ Graduate School of Advanced Integrated Studies in Human Survivability, Kyoto
8 University Yoshida–Nakaadachi–cho, Sakyo–ku, Kyoto, Japan

9 ² Hakubi Center for Advanced Research, Kyoto University, Yoshidahonmachi,
10 Sakyo–ku, Kyoto, Japan;

11 ³ Department of Population Health Sciences, School of Public Health, Georgia State
12 University, Atlanta, Georgia, USA

13 ⁴ Seto Marine Biological Laboratory, Field Science, Education and Research Center,
14 Kyoto University, Shirahama–cho, Nishimuro–gun, Wakayama 649–2211 Japan

15

16 §Corresponding author

17 Email addresses:

18 KM: mizumotokenji@gmail.com, KK: kagaya.katsushi.8e@kyoto-u.ac.jp, GC:

19 gchowell@gsu.edu

20 **Article type:**

21 Original Research

22 **Word count:**

23 Abstract: 350 (Max 350)

24 Main: 2768

25 **Abstract**

26 **Background:**

27 Since the first cluster of cases was identified in Wuhan City, China, in December, 2019,
28 coronavirus disease 2019 (COVID-19) has rapidly spread across China, causing
29 multiple introductions in 109 countries/territories/areas as of March 10th. Despite the
30 scarcity of publicly available data, scientists around the world have made strides in
31 estimating the magnitude of the epidemic, the basic reproduction number, and
32 transmission patterns. Recently more evidence suggests that a substantial fraction of the
33 infected individuals with the novel coronavirus show little if any symptoms, which
34 suggest the need to reassess the transmission potential of this emerging disease. In this
35 study, we derive estimates of the transmissibility and virulence of COVID-19 in Wuhan
36 City, China, by reconstructing the underlying transmission dynamics using multiple
37 data sources.

38 **Methods:**

39 We employ statistical methods and publicly available epidemiological datasets to jointly
40 derive estimates of transmissibility and severity associated with the novel coronavirus.
41 For this purpose, the daily series of laboratory–confirmed COVID-19 cases and deaths
42 in Wuhan City and epidemiological data of Japanese evacuees from Wuhan City on

43 board government–chartered flights were integrated into our analysis.

44 **Results:**

45 Our posterior estimates of basic reproduction number (R) in Wuhan City, China in
46 2019–2020 reached values as high as 5.20 (95%CrI: 5.04–5.47) and the enhanced public
47 health intervention after January 23rd in 2020 was associated with a declined R at 0.58
48 (95%CrI: 0.51–0.64), with the total number of infections (i.e. cumulative infections)
49 estimated at 1905526 (95%CrI: 1350283– 2655936) in Wuhan City, raising the
50 proportion of infected individuals to 19.1% (95%CrI: 13.5–26.6%). We also found that
51 most recent crude infection fatality ratio (IFR) and time–delay adjusted IFR is estimated
52 to be 0.04% (95% CrI: 0.03%–0.06%) and 0.12% (95%CrI: 0.08–0.17%), which is
53 several orders of magnitude smaller than the crude CFR estimated at 4.19%

54 **Conclusions:**

55 We have estimated key epidemiological parameters of the transmissibility and virulence
56 of COVID-19 in Wuhan, China during January-February, 2020 using an ecological
57 modelling approach. The power of our approach lies in the ability to infer
58 epidemiological parameters with quantified uncertainty from partial observations
59 collected by surveillance systems.

60 **Keywords:** epidemic; transmissibility; mathematical model; COVID-19; China

61

62 **Background**

63 The novel coronavirus (COVID-19) emerging from China is a deadly
64 respiratory pathogen that belongs to the same family as the coronavirus responsible for
65 the 2002-2003 Severe Acute Respiratory Syndrome (SARS) outbreaks [1]. Since the
66 first cluster of cases was identified in Wuhan City, China, in December, 2019,
67 COVID-19 has rapidly spread across China as well as caused multiple introductions in
68 109 countries/territories/areas as of March 10th, 2020 [2]. Nevertheless, China has been
69 hit hard by this emerging infectious disease, especially the city of Wuhan in Hubei
70 Province, where the first cluster of severe pneumonia caused by the novel virus was
71 identified. Meanwhile, the cumulative number of laboratory and clinically confirmed
72 cases and deaths in mainland China has reached 80778 and 3158, respectively, as of
73 March 10th, 2020 [3].

74 Because the morbidity and mortality burden associated with the novel
75 coronavirus has disproportionately affected the city of Wuhan, the center of the epidemic
76 in China, the central government of the People's Republic of China imposed a lockdown
77 and social distancing measures in this city and surrounding areas starting on January
78 23rd 2020. Indeed, out of the 80778 COVID-19 cases reported in China, 49978 cases
79 (61.9%) are from Wuhan City. In terms of the death count, a total of 2423 deaths
80 (76.7%) have been recorded in Wuhan city out of the 3158 deaths reported throughout
81 China. To guide the effectiveness of interventions, it is crucial to gauge the uncertainty
82 relating to key epidemiological parameters characterizing the transmissibility and the
83 severity of the disease. Despite the scarcity of publicly available data, scientists around
84 the world have made strides in estimating the magnitude of the epidemic, the basic
85 reproduction number, and transmission patterns [4-5]. Moreover, accumulating evidence

86 suggests that a substantial fraction of the infected individuals with the novel coronavirus
87 show little if any symptoms, which suggest the need to reassess the transmission
88 potential of this emerging disease [6]. For this purpose, in this study we employ
89 statistical methods and publicly available epidemiological datasets to jointly derive
90 estimates of transmissibility and severity associated with the novel coronavirus.

91

92 **Methods**

93 **Epidemiological data**

94 We linked our model to two different datasets. First, the daily series of
95 laboratory-confirmed nCov cases and deaths in Wuhan City were extracted according to
96 date of symptoms onset or reporting date from several sources [3, 7-8]. Our analysis
97 relies on epidemiological data reported prior to February 11th, 2020 because of the
98 change in case definition that was announced on February 12th, 2020 [9]. As of
99 February 11th, 2020, a total of 19559 confirmed cases including 820 deaths were
100 reported in Wuhan City. Second, epidemiological data of Japanese evacuees from
101 Wuhan City on board government-chartered flights were obtained from the Japanese
102 government. After arriving in Japan, all of the Japanese evacuees were kept in isolation
103 for about 14 days and examined for infection using polymerase chain reaction (PCR)
104 tests [7]. As of February 11th, a total of four flights with the Japanese evacuees left
105 Wuhan City. We collected information on the timing of the evacuee flights that left
106 Wuhan City as well as the number of passengers that tested positive for COVID-19 in
107 order to calibrate our model (Table S1).

108

109 **Statistical analysis**

110 Using the following integral equation model, we estimate the reproduction
111 number of COVID-19. Here, infected and reported cases are denoted by i and c ,
112 respectively.

113 We connected the daily incidence series with a discrete-time integral equation
114 to describe the epidemic dynamics. Let g_s denote the probability mass function of the
115 serial interval, e.g., the time from illness onset in a primary case to illness onset in the
116 secondary case, of length s days, which is given by

$$g_s = G(s) - G(s - 1) ,$$

117 For $s > 0$ where $G(\cdot)$ represents the cumulative distribution function of the gamma
118 distribution. Mathematically, we describe the expected number of new cases with day t ,
119 $E[c(t)]$ as follows,

$$E[c(t)] = \sum_{s=1}^{\infty} E[c(t-s)]R,$$

120 where $E[c(t)]$ represents the expected number of new cases with onset day t , where R
121 represents the average number of secondary cases per case.

122 Subsequently, we also employed the time-dependent variation in R to take into
123 account the impact of enhanced interventions on the transmission potential. This time
124 dependence was modelled by introducing a parameter δ_t , which is given by

$$\delta_t = \begin{cases} 1 & \text{otherwise} \\ \beta_1 & \text{if } t = \text{period}_1 \\ \beta_2 & \text{if } t = \text{period}_2 \end{cases}$$

125 where period_1 and period_2 represent the corresponding period from January 23rd to
126 February 2nd 2020 and from February 3rd to February 11th, 2020, respectively.
127 January 23rd 2020 is the date when the central government of the People's Republic of

128 China imposed a lockdown in Wuhan and other cities in Hubei in an effort to quarantine
129 the epicentre of the coronavirus (COVID-19) to mitigate transmission. Furthermore, we
130 evenly divide the interval into two periods to incorporate the time-dependent effects on
131 R using the parameters β_1 and β_2 which scale the extent of the intervention, taking
132 values smaller than 1 [10].

133 To account for the probability of occurrence, θ [11], we assume that the number
134 of observed cases on day t , $h(t)$, occurred according to a Bernoulli sampling process,
135 with the expected values $E(c_i; H_{t-1})$, where $E(c_i; H_{t-1})$ denotes the conditional expected
136 incidence on day t , given the history of observed data from day 1 to day $(t-1)$, denoted
137 by H_{t-1} . Thus, the number of expected newly observed cases is written as follows:

$$E[h(t); H_{t-1}] = \begin{cases} (1 - \theta) + \theta E[c(t); H_{t-1}], & \text{if } h = 0, \\ \theta E[c; H_{t-1}], & \text{otherwise,} \end{cases}$$

138 Further, we model the time-dependent variation in the reporting probability.
139 This time dependence was modelled by introducing a parameter δ_2 , which is given by

$$\delta_2 = \begin{cases} \alpha_1, & \text{if } t = \text{period}_3, \\ \alpha_2, & \text{if } t = \text{period}_4, \\ 1, & \text{otherwise,} \end{cases}$$

140 where period_3 and period_4 represent the corresponding periods from the start of our
141 study period to Jan 16 and from Jan 17 to Jan 22, respectively, while α_1 and α_2 scale the
142 extent of the reporting probability (where α_1 and α_2 is expected to be smaller than 1).
143 We evenly divide the duration before the lockdown was put in place into two to
144 incorporate the time dependency of the reporting probability. The number of expected
145 newly observed cases should be updated as

$$E[h(t); H_{t-1}] = \begin{cases} (1 - \theta) + q\delta\theta E[c(t); H_{t-1}], & \text{if } h_a = 0, \\ q\delta\theta E[c(t); H_{t-1}], & \text{otherwise,} \end{cases}$$

146 We assume the incidence, $h(t)$ is the result of the Binomial sampling process with the

147 expectation $E[h]$. The likelihood function for the time series of observed cases that we
148 employ to estimate the effective reproduction number and other relevant parameters is
149 given by:

$$L_1(U; c) = \prod_{t=1}^T \binom{E(h(t); H(t-1))}{c(t)} q^{c(t)} (1-q)^{E(h(t); H(t-1))-c(t)},$$

150 where U indicates parameter sets that are estimated from this likelihood.

151 Subsequently, the conditional probability of non-infection given residents in
152 Wuhan City at the time point of t_i , p_{t_i} , was assumed to follow a binomial distribution,
153 and the likelihood function is given by:

$$L_2(p_{t_i}; M_{t_i}, m_{t_i}) = \binom{M_{t_i}}{m_{t_i}} p_{t_i}^{m_{t_i}} (1-p_{t_i})^{M_{t_i}-m_{t_i}},$$

154 Where M_{t_i} and m_{t_i} is the number of government charted flight passengers and
155 non-infected passengers at the date of t_i , respectively, and p_{t_i} is the proportion of the
156 estimated non-infected population in Wuhan at the date of t_i , calculated from the $h(t)$
157 and catchment population in Wuhan City [3,13].

158 Serial interval estimates of COVID-19 were derived from previous studies of
159 nCov, indicating that it follows a gamma distribution with the mean and SD at 7.5 and
160 3.4 days, respectively, based on ref. [14]. The maximum value of the serial interval was
161 fixed at 28 days as the cumulative probability distribution of the gamma distribution up
162 to 28 days reaches 0.999.

163

164 **Infection fatality ratio**

165 Crude CFR and crude IFR is defined as the number of cumulative deaths
166 divided by the number of cumulative cases or infections at a specific point in time

167 without adjusting the time delay from illness onset or hospitalization to death. Next, we
 168 employed an integral equation model in order to estimate the real-time IFR. First, we
 169 estimated the real-time CFR as described elsewhere [15-17]. For the estimation, we
 170 employ the delay from hospitalization to death, f_s , which is assumed to be given by $f_s =$
 171 $F(s) - F(s-1)$ for $s > 0$ where $H(s)$ follows a gamma distribution with mean 10.1 days and
 172 SD 5.4 days, obtained from the available observed data [18].

$$L_3(\pi; c_t, \theta) = \prod_{t_i} \binom{t_i}{D_{t_i}} \left(\pi \frac{\sum_{t=2}^{t_i} \sum_{s=1}^{t-1} c_{t-s} f_s}{\sum_{t=1}^{t_i} c_t} \right)^{D_{t_i}} \left(1 - \pi \frac{\sum_{t=2}^{t_i} \sum_{s=1}^{t-1} c_{t-s} f_s}{\sum_{t=1}^{t_i} c_t} \right)^{\sum_{t=1}^{t_i} c_t - D_{t_i}}$$

173 where c_t represents the number of new cases with reported day t , and D_{t_i} is the number
 174 of new deaths with reported day t_i [16-18]. We assume that the cumulative number of
 175 observed deaths, D_t is the result of the binomial sampling process with probability π .
 176 Subsequently, crude IFR and time-delay adjusted IFR are calculated using the estimated
 177 π and h_t .

178 The total likelihood is calculated as $L=L_1L_2L_3$ and model parameters were
 179 estimated using a Monte Carlo Markov Chain (MCMC) method in a Bayesian
 180 framework. Posterior distributions of the model parameters were estimated based on
 181 sampling from the three Markov chains. For each chain, we drew 100,000 samples from
 182 the posterior distribution after a burn-in of 20,000 iterations. Convergence of MCMC
 183 chains were evaluated using the potential scale reduction statistic [19-20]. Estimates and
 184 95% credibility intervals for these estimates are based on the posterior probability

185 distribution of each parameter and based on the samples drawn from the posterior
186 distributions. All statistical analyses were conducted in R version 3.5.2 (R Foundation
187 for Statistical Computing, Vienna, Austria) using the ‘rstan’ package.

188

189 **Results**

190 The daily series of COVID-19 laboratory–confirmed incidence and cumulative
191 incidence in Wuhan in 2019–2020 are displayed in Figure 1. Overall, our dynamical
192 models yield a good fit to the temporal dynamics (i.e. incidence, cumulative incidence)
193 including an early exponential growth pattern in Wuhan. In incidence data, a few
194 fluctuations are seen, probably indicating that the surveillance system likely missed
195 many cases during the early transmission phase (Figure 1).

196 Our posterior estimates of basic reproduction number (R) in Wuhan City, China
197 in 2019–2020 was estimated to be as high as 5.20 (95%CrI: 5.04–5.47). The
198 time–dependent scaling factors quantifying the extent of enhanced public health
199 intervention on R is 0.99 (95%CrI: 0.94–1.00), declining R to 5.12 (95%CrI: 4.98–5.26)
200 from January 23rd to February 1st and 0.11 (95%CrI: 0.10–0.13), declining R to 0.58
201 (95%CrI: 0.51–0.64) from February 2nd to February 11th, 2020. Other parameter
202 estimates for the probability of occurrence and reporting rate are 0.97 (95% CrI:
203 0.84–1.00) and 0.010 (95% CrI: 0.007–0.014), respectively. Moreover, the
204 time–dependent scaling factor quantifying the extent of reporting rate, α , is estimated to
205 be 0.08 (95% CrI: 0.03–0.19) before January 16th and to be 0.99 (95% CrI: 0.96–1.00)
206 from January 17th to January 22nd.

207 The total number of estimated laboratory–confirmed cases (i.e. cumulative
208 cases) is 18913 (95% CrI: 16444–19705) while the actual numbers of reported

209 laboratory-confirmed cases during our study period is 19559 as of February 11th, 2020.
210 Moreover, we inferred the total number of COVID-19 infections (Figure S1). Our
211 results indicate that the total number of infections (i.e. cumulative infections) is
212 1905526 (95%CrI: 1350283– 2655936).

213 The Observed and posterior estimates of the cumulative number of deaths from
214 COVID-19 in Wuhan are displayed in Figure 2, and model-based posterior estimates of
215 the cumulative number of deaths is 820 (95%CrI: 744–900), while actual number of
216 reported deaths is 820. The estimated temporal variation in the death risk caused by
217 COVID-19 in Wuhan, China, 2019–2020 is shown in Figure 3 and Figure S2. Observed
218 and posterior estimated of crude CFR in Wuhan City is presented in Figure 2A, while
219 observed and posterior estimates of time-delay adjusted CFR is shown in Figure 2B.
220 Furthermore, Figure 3A and 3B illustrates time-delay no-adjusted IFR and time-delay
221 adjusted IFR, respectively.

222 The latest estimate of the crude CFR and time-delay adjusted CFR in Wuhan
223 appeared to be 4.2% (95% CrI: 3.9–4.9%) and 12.2% (95% CrI: 11.4–13.0%),
224 respectively, whereas the latest model-based posterior estimates of time-delay not
225 adjusted IFR and adjusted IFR, presented in Figure 3 C and D, are 0.04%(95% CrI:
226 0.03%–0.06%) and 0.12% (95%CrI: 0.08–0.17%), respectively, while the observed
227 crude CFR is calculated to be 4.19% (Table 1).

228

229 **Discussion**

230 In this study we derived estimates of the transmissibility and virulence of
231 COVID-19 in Wuhan City, China, by reconstructing the underlying transmission

232 dynamics using multiple data sources. Applying dynamic modeling, the reproduction
233 number and death risks as well as probabilities of occurrence and reporting rate were
234 estimated.

235 Our posterior estimates of basic reproduction number (R) in Wuhan City, China
236 in 2019–2020 is calculated to be as high as 5.20 (95%CrI: 5.04–5.47). The
237 time–dependent scaling factor quantifying the extent of enhanced public health
238 intervention on R is 0.99 (95%CrI: 0.94–1.00), declining R to 5.12 (95%CrI: 4.98–5.26)
239 from January 23rd to February 1st and 0.11 (95%CrI: 0.10–0.13), declining R to 0.58
240 (95%CrI: 0.51–0.64) for February 2nd to February 11th, 2020. These R estimates
241 capturing the underlying transmission dynamics modify the impact of COVID-19, with
242 the total number of infections (i.e. cumulative infections) estimated at 1905526
243 (95%CrI: 1350283– 2655936) in Wuhan City, raising the proportion of infected
244 individuals to 19.1% (95%CrI: 13.5–26.6%) with a catchment population in Wuhan
245 City of 10 million people. Our estimates of mean reproduction number reached values
246 as high as 5.20, an estimate that is slightly higher than previous mean estimates in the
247 range 2.2-3.8 derived by fitting epidemic models to the initial growth phase of the
248 observed case incidence [21-23]. By comparison, the R estimate for the Diamond
249 Princess cruise ship in Japan reached values as high as ~11 [24]. Further, these estimates
250 are higher than recent mean R estimates derived from the growth rates of the COVID-19
251 outbreaks in Singapore ($R\sim 1.1$) [25] and Korea ($R\sim 1.5$) [26].

252

253 The sustained high R values in Wuhan City even after the lockdown and mobility
254 restrictions suggests that transmission is occurring inside the household or amplified in
255 healthcare settings [18], which is a landmark of past SARS and MERS outbreaks

256 [27-28]. Considering the potent transmissibility of COVID-19 in confined settings, as
257 illustrated by COVID-19 outbreaks aboard cruise ships, including the Diamond Princess
258 cruise ship, where the total number of secondary or tertiary infections reached 705
259 among more than 3,700 passengers as of February 28th, 2020 and also by the COVID-19
260 outbreak tied to the Shincheonji religious sect in South Korea where church members
261 appear to have infected from seven to 10 people. [29-31], it is crucial to prevent
262 transmission in confined settings including hospital-based transmission by
263 strengthening infection control measures as well as transmission stemming from large
264 social gatherings.

265 Our most recent estimates of the crude CFR and time-delay adjusted CFR are
266 at 4.2% (95% CrI: 3.9–4.9%) and 12.23% (95% CrI: 11.4–13.0%), respectively. In
267 contrast, our most recent crude IFR and time-delay adjusted IFR is estimated to be
268 0.04% (95% CrI: 0.03%–0.06%) and 0.12% (95%CrI: 0.08–0.17%), which is several
269 orders of magnitude smaller than the crude CFR at 4.19%. These findings indicate that
270 the death risk in Wuhan is estimated to be much higher than those in other areas, which
271 is likely explained by hospital-based transmission [32]. Indeed, past nosocomial
272 outbreaks have been reported to elevate the CFR associated with MERS and SARS
273 outbreaks, where inpatients affected by underlying disease or seniors infected in the
274 hospital setting have raised the CFR to values as high as 20% for a MERS outbreak
275 [33-34].

276 Public health authorities are interested in quantifying R and CFR to measure
277 the transmission potential and virulence of an infectious disease, especially when
278 emerging/re-emerging epidemics occur in order to decide the intensity of the public
279 health response. In the context of a substantial fraction of unobserved infections due to

280 COVID-19, R estimates derived from the trajectory of infections and the IFR are more
281 realistic indicators compared to estimates derived from observed cases alone [18,
282 35-36].

283 Our analysis also revealed a high probability of occurrence and quite low
284 reporting probabilities in Wuhan City. High probability of occurrence in the above
285 equation suggests that zero observed cases at some point is not due to the absence of
286 those infected, but more likely due to a low reporting rate. A very low reporting
287 probability suggests that it is difficult to diagnose COVID-19 cases or a breakdown in
288 medical care delivery. Moreover, we also identified a remarkable change in the
289 reporting rate, estimated to be 12-fold lower in the 1st period (–Jan 16, 2020) and about
290 the same during the 2nd period (January 17th – 22nd, 2020), relative to the that
291 estimated after January 23rd 2020.

292

293 Our results are not free from the limitations. First, our methodology aims to capture the
294 underlying transmission dynamics using multiple data sources. By implementing mass
295 screening in certain populations is a useful approach to ascertain the real proportion of
296 those infected and a way of adding credibility to the estimated values. Second, it is
297 worth noting that the data of Japanese evacuee employed in our analysis is not a random
298 sample from the Wuhan catchment population. Indeed, it also plausible that their risk of
299 infection in this sample is not as high as that of local residents in Wuhan,
300 underestimating the fatality risk.

301 **Conclusion**

302 In summary, we have estimated key epidemiological parameters of the

303 transmissibility and virulence of COVID-19 in Wuhan, China, January-February, 2020
304 using an ecological modelling approach and several epidemiological datasets. The
305 power of our approach lies in the ability to infer epidemiological parameters with
306 quantified uncertainty from partial observations collected by surveillance systems.
307

308 **List of abbreviations**

309 CFR: Case fatality ratio, IFR: Infection Fatality ratio, SARS: Severe Acute Respiratory
310 Syndrome, MERS: Middle East Respiratory Syndrome
311

312 **Additional files**

313 **Additional file 1:**

314 **Appendix. Table S1.** Information related to Japanese evacuees from Wuhan City on
315 board government-chartered flights
316
317

318 **Declarations**

319 **Ethics approval and consent to participate**

320 Not applicable.

321 **Consent for publication**

322 Not applicable.

323 **Availability of data and materials**

324 The present study relies on published data and access information to essential
325 components of the data are available from the corresponding author.

326 **Competing interests**

327 The authors declare that they have no competing interests.

328

329 **Funding**

330 KM acknowledges support from the Japan Society for the Promotion of Science (JSPS)

331 KAKENHI Grant Number 18K17368 and from the Leading Initiative for Excellent

332 Young Researchers from the Ministry of Education, Culture, Sport, Science &

333 Technology of Japan. KK acknowledges support from the JSPS KAKENHI Grant

334 Number 18K19336 and 19H05330. GC acknowledges support from NSF grant 1414374

335 as part of the joint NSF–NIH–USDA Ecology and Evolution of Infectious Diseases

336 program.

337 **Authors' contributions**

338 KM and GC conceived the early study idea. KM and KK built the model. KM
339 implemented statistical analysis and wrote the first full draft. GC advised on and helped
340 shape the research. All authors contributed to the interpretation of the results and edited
341 and commented on several earlier versions of the manuscript.

342 **Acknowledgements**

343 Not applicable.

344

345 **REFERENCES**

346 1. Jon Cohen. **Mining coronavirus genomes for clues to the outbreak's origins.**

347 **Science.** Jan 31, 2020.

348 <https://www.sciencemag.org/news/2020/01/mining-coronavirus-genomes-clues->

349 [outbreak-s-origins.](https://www.sciencemag.org/news/2020/01/mining-coronavirus-genomes-clues-) Accessed, 3 Feb, 2020

350 2. World Health Organization (WHO). Novel Coronavirus (2019-nCoV) situation

351 reports. Available from:

352 <https://www.who.int/emergencies/diseases/novel-coronavirus-2019/situation-rep>

353 [orts](https://www.who.int/emergencies/diseases/novel-coronavirus-2019/situation-rep) Accessed, [cited 2020 Mar 10]

- 354 3. The State Council, The People's Republic of China. [cited 2020 Mar 10].
355 <http://www.gov.cn/>
- 356 4. Nishiura H, Jung SM, Linton NM, Kinoshita R, Yang Y, Hayashi K, et al. **The**
357 **Extent of Transmission of Novel Coronavirus in Wuhan, China, 2020.** *J Clin*
358 *Med.* 2020; 9(2); 330
- 359 5. Wu JT, Leung K, Leung GM. **Nowcasting and forecasting the potential**
360 **domestic and international spread of the 2019-nCoV outbreak originating**
361 **in Wuhan, China: a modelling study.** *Lancet.* 2020. pii:
362 S0140-6736(20)30260-9. doi: 10.1016/S0140-6736(20)30260-9.
- 363 6. Linton NM, Kobayashi T, Yang Y, Hayashi K, Akhmetzhanov AR, Jung SM, et
364 al. **Epidemiological characteristics of novel coronavirus infection: A**
365 **statistical analysis of publicly available case data.** *medRxiv*
366 2020.01.26.20018754; doi: <https://doi.org/10.1101/2020.01.26.20018754>
- 367 7. Health Commission of Hubei Province, China. [cited 2020 Feb 7].
368 <http://wjw.hubei.gov.cn/>
- 369 8. Health Commission of Wuhan City, Hubei Province, China [cited 2020 Feb 7]
370 <http://wjw.hubei.gov.cn/>

- 371 9. Clinical guideline for COVID-19, version 5. The State Council, The People's
372 Republic of China. Available from
373 <http://www.gov.cn/zhengce/zhengceku/2020-02/05/5474791/files/de44557832a>
374 [d4be1929091dcbcfca891.pdf](http://www.gov.cn/zhengce/zhengceku/2020-02/05/5474791/files/de44557832a) [Accessed Feb/29, 2020][in Chinese]
- 375 10. Ministry of Health, Labour and Welfare, Japan.
376 <https://www.mhlw.go.jp/index.html> [in Japanese]
- 377 11. 2020 Hubei lockdowns, Wikipedia.
378 https://en.wikipedia.org/wiki/2020_Hubei_lockdowns
- 379 12. Li R,a Weiskittel AR,a Kershaw Jr, JA. **Modeling annualized occurrence,**
380 **frequency, and composition of ingrowth using mixed-effects zero-inflated**
381 **models and permanent plots in the Acadian Forest Region of North**
382 **America.** *Can J For Res.* 2011; 41:2077–2089
- 383 13. Northeastern University. Laboratory for the Modeling of Biological and Socio -
384 Technical Systems, 2020. Available online: [https://www.mobs -](https://www.mobs-lab.org/2019ncov.html)
385 [lab.org/2019ncov.html](https://www.mobs-lab.org/2019ncov.html) (accessed on 22 January 2020).
- 386 14. Huang C, Wang Y, Li X, et al. **Clinical features of patients infected with 2019**
387 **novel coronavirus in Wuhan, China.** *Lancet.* 2020. pii:
388 S0140-6736(20)30183-5.

- 389 15. Ghani AC, Donnelly CA, Cox DR, Griffin JT, Fraser C, Lam TH, et al.
390 **Methods for estimating the case fatality ratio for a novel, emerging**
391 **infectious disease.** *Am J Epidemiol.* 2005; 162: 479-486
- 392 16. Nishiura H, Klinkenberg D, Roberts M, Heesterbeek JA. **Early epidemiological**
393 **assessment of the virulence of emerging infectious diseases: a case study of**
394 **an influenza pandemic.** *PLoS One.* 2009;4(8):e6852. doi:
395 10.1371/journal.pone.0006852.
- 396 17. Tsuzuki S, Lee H, Miura F, Chan YH, Jung SM, Akhmetzhanov AR, Nishiura H.
397 **Dynamics of the pneumonic plague epidemic in Madagascar, August to**
398 **October 2017.** *Euro Surveill.* 2017;22(46). doi:
399 10.2807/1560-7917.ES.2017.22.46.17-00710.
- 400 18. Mizumoto K, Chowell G. **Estimating the risk of 2019 Novel Coronavirus**
401 **death during the course of the outbreak in China, 2020.** *Emerg Infect Dis.*
402 2020. Accepted.
- 403 19. Gamerman, D. & Lopes, H. F. **Markov Chain Monte Carlo: Stochastic**
404 **Simulation for Bayesian Inference.** 2nd edn (Chapman & Hall/CRC, 2006).
- 405 20. Gelman, A. & Rubin, D. B. **Inference from iterative simulation using**
406 **multiple sequences.** *Stat Sci* 7:457-472, doi:10.1214/ss/1177011136 (1992).

- 407 21. Li Q, Guan X, et. al. **Early Transmission Dynamics in Wuhan, China, of**
408 **Novel Coronavirus–Infected Pneumonia.** *N Engl J Med.* 2020 Jan 29. DOI:
409 10.1056/NEJMoa2001316 Available at:
410 <https://www.nejm.org/doi/full/10.1056/NEJMoa2001316>
- 411 22. Read JM, Bridgen JR, Cummings DA, Ho A, Jewell CP. **Novel coronavirus**
412 **2019-nCoV: early estimation of epidemiological parameters and epidemic**
413 **predictions.** *medRxiv.* doi: <https://doi.org/10.1101/2020.01.23.20018549>
- 414 23. Imai N, Cori A, Dorigatti I, Baguelin M, Donnelly CA, Riley S, Ferguson NM.
415 **Report 3: Transmissibility of 2019-nCoV.**
416 [https://www.imperial.ac.uk/media/imperial-college/medicine/sph/ide/gida-fello](https://www.imperial.ac.uk/media/imperial-college/medicine/sph/ide/gida-fellowships/Imperial-2019-nCoV-transmissibility.pdf)
417 [wships/Imperial-2019-nCoV-transmissibility.pdf](https://www.imperial.ac.uk/media/imperial-college/medicine/sph/ide/gida-fellowships/Imperial-2019-nCoV-transmissibility.pdf)
- 418 24. Mizumoto K, Chowell G. **Transmission potential of the novel coronavirus**
419 **(COVID-19) onboard the Diamond Princess Cruises Ship, 2020.** *Infect Dis*
420 *Model.* 2020. 264-270
- 421 25. Tariq A, Lee Y, Roosa K, Blumberg S, Yan P, Ma S, Chowell G. **Real-time**
422 **monitoring the transmission potential of COVID-19 in Singapore, February**
423 **2020.** *medRxiv.* doi: <https://doi.org/10.1101/2020.02.21.20026435>

- 424 26. Shim E, Tariq A, Choi W, Lee Y, Chowell G. **Transmission potential of**
425 **COVID-19 in South Korea.** *medRxiv*.
426 doi:<https://doi.org/10.1101/2020.02.27.20028829>
- 427 27. Chowell G, Abdirizak F, Lee S, Lee J, Jung E, Nishiura H, Viboud C.
428 **Transmission characteristics of MERS and SARS in the healthcare setting:**
429 **a comparative study.** *BMC Med.* 2015;**13**:210. doi:
430 10.1186/s12916-015-0450-0.
- 431 28. Abdirizak F, Lewis R, Chowell G. **Evaluating the potential impact of targeted**
432 **vaccination strategies against severe acute respiratory syndrome**
433 **coronavirus (SARS-CoV) and Middle East respiratory syndrome**
434 **coronavirus (MERS-CoV) outbreaks in the healthcare setting.** *Theor Biol*
435 *Med Model.* 2019;**16**(1):16. doi: 10.1186/s12976-019-0112-6.
- 436 29. Blake Essig, Brent Swails, Yoko Wakatsuki and Ben Westcott, CNN. **Top**
437 **Japanese government adviser says Diamond Princess quarantine was**
438 **flawed.** Updated 0708 GMT (1508 HKT) February 27, 2020.
439 <https://edition.cnn.com/2020/02/27/asia/japan-diamond-princess-quarantine-cre>
440 [w-intl-hnk/index.html](https://edition.cnn.com/2020/02/27/asia/japan-diamond-princess-quarantine-cre-w-intl-hnk/index.html)

- 441 30. Da-hae P, Dam-eun S, Jae-gu K. HANKYOREH. **The reasons why**
442 **transmission is so prevalent among Shincheonji members.** Mar 2, 2020.
443 http://english.hani.co.kr/arti/english_edition/e_national/930749.html [Accessed
444 Mar/10, 2020]
- 445 31. Mizumoto K, Kagaya K, Zarebski A, Chowell G. **Estimating the**
446 **Asymptomatic Proportion of 2019 Novel Coronavirus onboard the Princess**
447 **Cruises Ship, 2020.** *Euro Surveill.* 2020. Accepted.
- 448 32. Wang D, Hu B, Hu C, Zhu F, Liu X, Zhang J, et al. **Clinical Characteristics of**
449 **138 Hospitalized Patients With 2019 Novel Coronavirus-Infected**
450 **Pneumonia in Wuhan, China.** *JAMA.* 2020. doi: 10.1001/jama.2020.1585.
- 451 33. Mizumoto K, Endo A, Chowell G, Miyamatsu Y, Saitoh M, Nishiura H.
452 **Real-time characterization of risks of death associated with the Middle East**
453 **respiratory syndrome (MERS) in the Republic of Korea, 2015.** *BMC Med.*
454 2015;**13**:228. doi: 10.1186/s12916-015-0468-3.
- 455 34. Mizumoto K, Saitoh M, Chowell G, Miyamatsu Y, Nishiura H. **Estimating the**
456 **risk of Middle East respiratory syndrome (MERS) death during the course**
457 **of the outbreak in the Republic of Korea, 2015.** *Int J Infect Dis.* 2015;**39**:7-9.
458 doi: 10.1016/j.ijid.2015.08.005.

- 459 35. J.Y. Wong, P. Wu, H. Nishiura, E. Goldstein, E.H. Lau, L. Yang, et al. **Infection**
460 **fatality risk of the pandemic A(H1N1)2009 virus in Hong Kong.** *Am J*
461 *Epidemiol.* 2013;**177 (8)**:pp. 834-840
- 462 36. Presanis AM, De Angelis D; New York City Swine Flu Investigation Team,
463 Hagy A, Reed C, Riley S, Cooper BS, et al. **The severity of pandemic H1N1**
464 **influenza in the United States, from April to July 2009: a Bayesian analysis.**
465 *PLoS Med.* 2009;**6(12)**:e1000207.
466

467 **Figures**

468 **Figure 1. Observed and posterior estimates of the daily new cases and**

469 **cumulative cases of the COVID-19 cases in Wuhan, China, 2019–2020**

470 Observed and posterior estimates of laboratory–confirmed reported cases (A) and

471 cumulative reported cases (B) are presented.

472 Observed data are presented in the dot, while dashed line indicates 50 percentile, and

473 areas surrounded by light grey and deep grey indicates 95% and 50% credible intervals

474 (CrI) for posterior estimates, respectively. Epidemic day 1 corresponds to the day that

475 starts at January 1st, 2020.

476

477 **Figure 2. Observed and posterior estimates of the cumulative deaths of the**

478 **COVID-19 in Wuhan, China, 2019–2020**

479 Observed and posterior estimates of the cumulative deaths of the COVID-19 in Wuhan

480 is presented. Observed data are presented in the dot, while dashed line indicates 50

481 percentile, and areas surrounded by light grey and deep grey indicates 95% and 50%

482 credible intervals (CrI) for posterior estimates, respectively. Epidemic day 1

483 corresponds to the day that starts at January 1st, 2020.

484

485 **Figure 3. Temporal variation of the infection fatality risks caused by COVID-19 in**

486 **Wuhan, China, 2019–2020**

487

488 (A) Posterior estimates of crude infection fatality ratio in Wuhan City. (B) Posterior
489 estimates of time–delay adjusted infection fatality ratio in Wuhan City.
490 Black dots shows observed data, and light and dark indicates 95% and 50% credible
491 intervals for posterior estimates, respectively. Epidemic day 1 corresponds to the day
492 that starts at January 1st, 2020.
493

494 **Figure S1. Observed daily new cases and posterior estimates of the daily new**

495 **infections of the COVID-19 in Wuhan, China, 2019–2020**

496 Observed daily new cases and posterior estimates of infections of the COVID-19 are
497 presented.

498 Observed data are presented in the dot, while dashed line indicates 50 percentile, and
499 areas surrounded by light grey and deep grey indicates 95% and 50% credible intervals
500 (CrI) for posterior estimates, respectively. Epidemic day 1 corresponds to the day that
501 starts at January 1st, 2020.

502

503 **Figure S2. Temporal variation of the case fatality risks caused by COVID-19 in**
504 **Wuhan, China, 2019–2020**

505 (A) Observed and posterior estimates of crude case fatality ratio in Wuhan City, (B)

506 Observed crude case fatality ratio and posterior estimates of time–delay adjusted CFR
507 in Wuhan City.

508 This figure is submitted to the ref [18]. The purpose of the study is to compare the case
509 fatality ration (CFR. Not IFR) in three different areas (Wuhan City, in Hubei Province
510 excluding Wuhan City and in China excluding Hubei Province) to interpret the current
511 severity of the epidemic in China, and the purpose is different from this study.

512

513

514 **Tables**

515 Table 1 – Death risk by COVID-19 in Wuhan City, China, 2020 (As of
516 February 12, 2020)

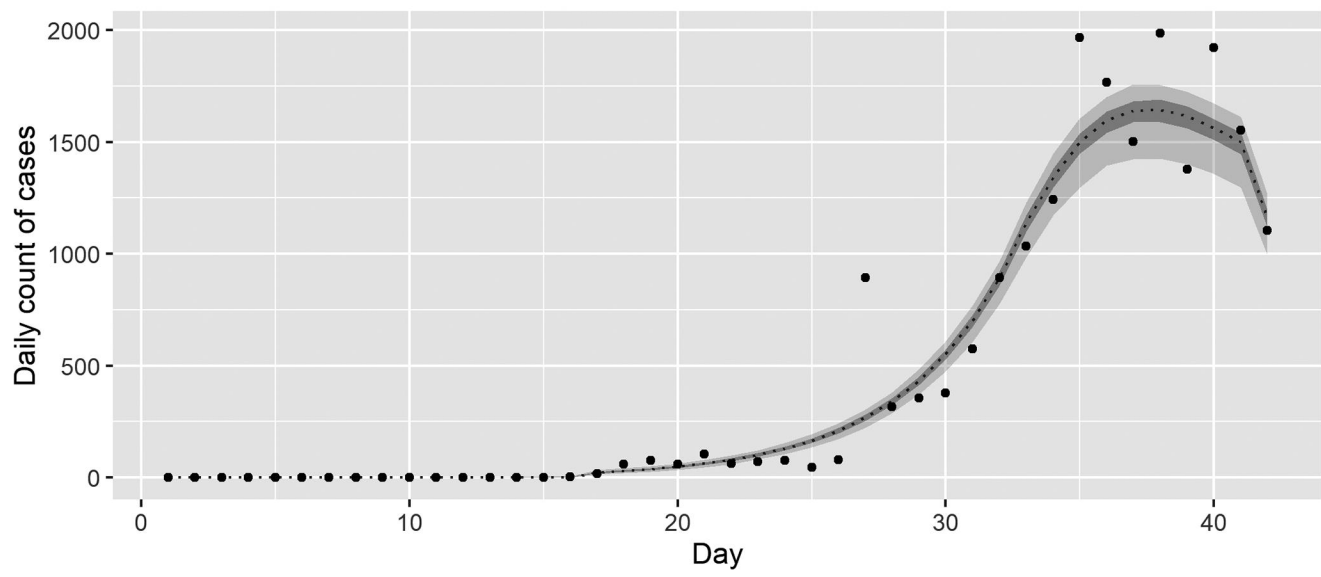
Death Risk	Latest estimate	Range of median estimates
Crude CFR (Observed)	4.19%	2.0 – 9.0%
Crude CFR (Estimated)	4.2% (95%CrI [‡] : 3.9 – 4.9%)	3.4 – 7.2%
Time delay adjusted CFR	12.2% (95%CrI: 11.4 – 13.0%)	4.1 – 34.8%
Crud IFR	0.04% (95%CrI: 0.03 – 0.06%)	0.02 – 0.07%
Time delay adjusted IFR	0.12% (95%CrI: 0.08 – 0.17%)	0.04 – 0.33%

517 CrI: Credibility intervals, CFR: Case fatality ratio, IFR: Infection fatality
518 ratio

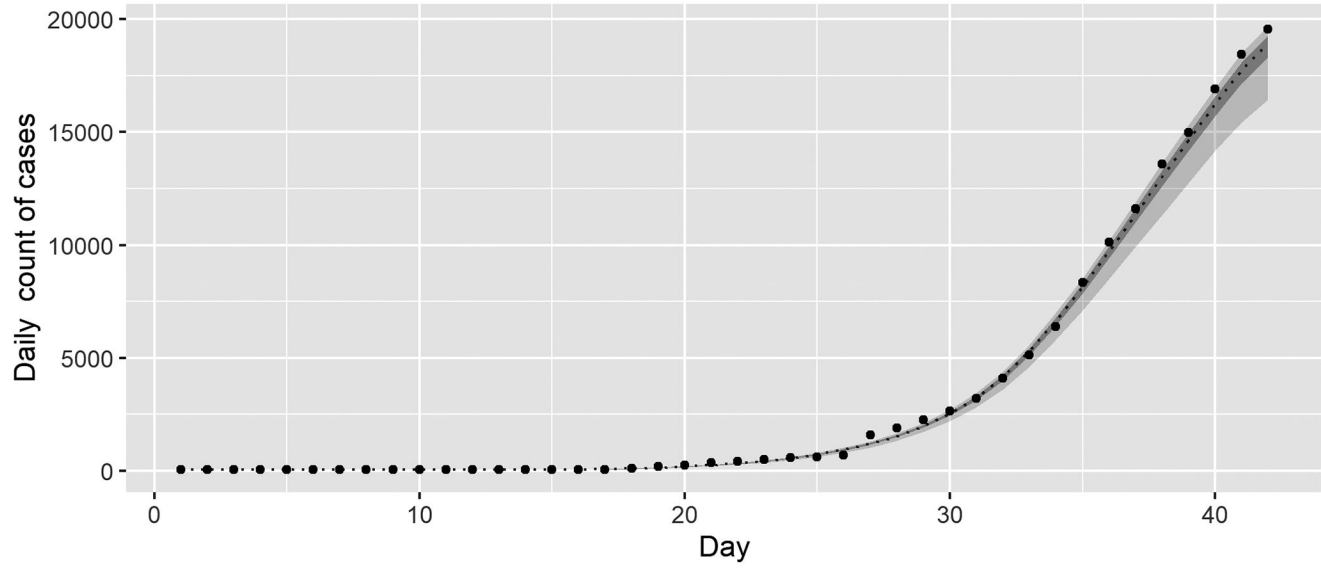
519 [‡]Upper and lower 95% credibility interval

520

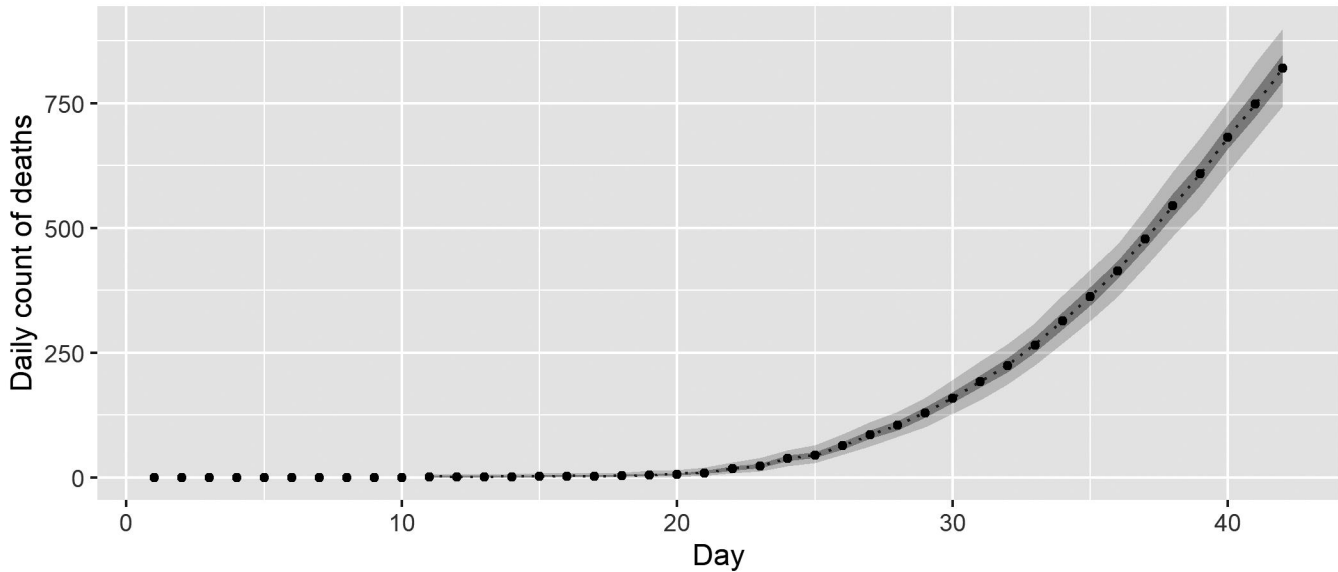
A Observed and estimated number of reported cases
Wuhan



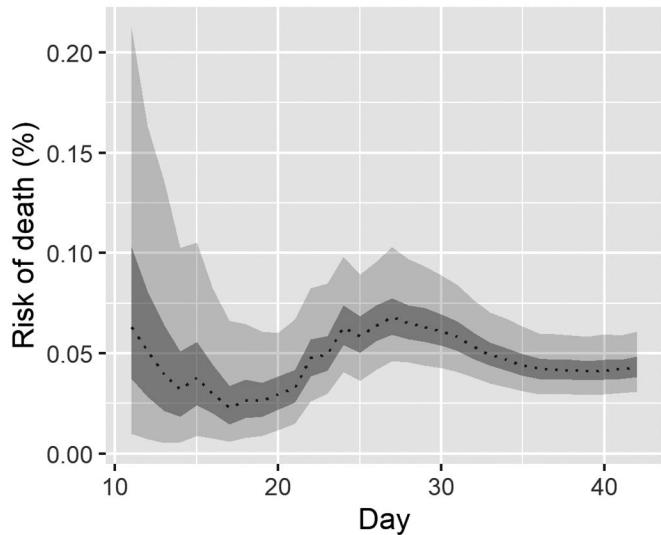
B Observed and estimated number of cumulative reported cases
Wuhan



Observed and estimated number of reported cumulative death Wuhan



A Infection fatality ratio
Crude
Wuhan



B Infection fatality ratio
Time-delay adjusted
Wuhan

